PHYSICAL REVIEW E **72**, 040201(R) (2005)

Monte Carlo simulation of a model of water

A. C. Maggs
Laboratoire de Physico-Chime Théorique, UMR CNRS-ESPCI 7083, 10 rue Vauquelin, 75231 Paris Cedex 05, France
(Received 13 June 2005; published 14 October 2005)

We simulate TIP3P water using a constrained Monte Carlo algorithm to generate electrostatic interactions eliminating the need to sum over long-ranged Coulomb interactions. We study discretization errors when interpolating charges using splines and Gaussians. We compare our implementation to molecular dynamics and Brownian dynamics codes.

DOI: 10.1103/PhysRevE.72.040201 PACS number(s): 61.20.Ja, 07.05.Tp, 71.15.Pd, 72.20.Jv

The TIP3P model of water [1] is often used to study the accuracy of algorithms for atomistic simulation. The model has a single Lennard-Jones center representing an oxygen atom together with three charges $(-0.834, +0.417, +0.417)$ arranged in a triangle. The oxygen-hydrogen bond length is 0.9572 Å the angle between bonds is 104.52°. Accurate simulation of this model is surprisingly challenging: The bare electrostatic interaction between oxygen atoms at a separation of 2.75 Å, is over 100 k_BT. Small errors in the representation of the electrostatic potential lead to significant errors in the total energy due to large cancellations; the binding energy per hydrogen bond is only 7 k_BT.

Many molecular dynamics codes for the simulation of large numbers of charges are based on Poisson solvers. The codes interpolate charges to a cubic grid and then calculate the electrostatic energy via fast Fourier transform [2] or multigrid [3,4]. The principle difficulty is controlling errors in the Coulomb interaction using high-order interpolation. One requires a relative error of at most $\sim 10^{-4}$. In this article, we present a Monte Carlo algorithm for simulation at this level of accuracy. We avoid solving the Poisson equation by generalizing an algorithm which generates the Coulomb interaction between particles using Monte Carlo evolution of the electric field. Previous codes using this local algorithm have been of low accuracy, sufficient for the study of lattice gasses [5,6] or charges interacting through an implicit solvent [7,8]. They were still far from the accuracy needed for the simulation of TIP3P. This articles considers the modifications necessary to the algorithm in order to reliably simulate standard atomistic models.

There were three important sources of error in the energy functions used in previous work with local electrostatics algorithms: [8]

(i) Use of low-order interpolation leading to distorted charge distributions.

(ii) Aliasing errors in the lattice Green functions leading to a self-energy with the periodicity of the lattice.

(iii) Low-order discretization of the lattice Green function leading to anisotropy in the effective interactions.

In many codes, interpolation of charges from the continuum to the cubic grid is performed with splines. A one-dimension n-spine is a set of n polynomials of order $n-1$. These polynomials give the quantity of charge which is deposited on n consecutive sites of the lattice as a function of the position of the particle, $f_i(x)$, $1 \leqslant i \leqslant n$. Linear interpolation corresponds to a two-spline. In three dimensions, one takes the product of splines in the x, y, and z directions, interpolating a charge to n^3 lattice site, thus $f_{\mathbf{l}}(\mathbf{r}) = f_i(x) f_j(y) f_k(z)$ for $\mathbf{r}=(x,y,z)$ and $\mathbf{l}=(i,j,k)$. Splines have several useful properties for interpolation: They conserve total charge exactly; they are smooth with $n-2$ continuous derivatives. With Fourier solvers splines work well if one takes $n \geqslant 4$ [2].

An alternative to splines is interpolation with truncated Gaussians [2,3]. Consider interpolating a unit charge to a one-dimensional grid with Gaussian interpolation: $f_i(x) = \exp(-(x-i)^2/2\sigma^2)/\sqrt{2\pi\sigma}$. The total interpolated charge can be evaluated for σ large with the Poisson re-summation formula: $q_{\text{int}} = \Sigma_i f_i(x) = \Sigma_p \tilde{f}(2\pi p)$ where $\tilde{f}$ is the (continuous) Fourier transform of $f_i(x)$. We find $q_{\text{int}} \sim 1 + 2\cos(2\pi x) e^{-2\pi^2\sigma^2}$. Already for $\sigma = 1$, errors in charge conservation are $O(10^{-8})$. In practice, one truncates beyond $\lambda\sigma$, where $\lambda \sim 4-5$, leading to an additional error which varies as $e^{-\lambda^2/2}$.

In order to study the various errors generated with lattice Monte Carlo algorithms for the electrostatic energy, consider the interaction between two particles placed at $\mathbf{r}$ and $\mathbf{r}'$.

$$U(\mathbf{r},\mathbf{r}') = \sum_{\mathbf{l},\mathbf{m}} f_{\mathbf{l}}(\mathbf{r}) G(\mathbf{l}-\mathbf{m}) f_{\mathbf{m}}(\mathbf{r}'), \tag{1}$$

$$= \sum_{\mathbf{p}} \int \frac{d^3\mathbf{q}}{(2\pi)^3} \tilde{f}(\mathbf{q} - 2\pi\mathbf{p}) \tilde{f}(\mathbf{q}) G(\mathbf{q}) \times e^{i\mathbf{q}\cdot(\mathbf{r}-\mathbf{r}') + 2\pi i \mathbf{p}\cdot\mathbf{r}}, \tag{2}$$

where $G(\mathbf{l})$ is the lattice Green function of the interaction between two sites and $G(\mathbf{q})$, its Fourier transform, has the periodicity of the Brillouin zone. $2\pi\mathbf{p}$ is a vector of the reciprocal lattice. The integral is over all Fourier space. The particles also have a self-energy $U(\mathbf{r},\mathbf{r})/2$.

Consider the contribution $\mathbf{p}=0$ in Eq. (2)

$$U_0(\mathbf{r},0) = \int G(\mathbf{q}) \tilde{f}^2(\mathbf{q}) e^{i\mathbf{q}\cdot\mathbf{r}} \frac{d^3\mathbf{r}}{(2\pi)^3}. \tag{3}$$

If $\tilde{f}$ is Gaussian and $G(r) = 1/4\pi r$, $G(q) = 1/q^2$ so that

$$U_0(\mathbf{r},0) + \frac{\mathrm{erfc}(r/2\sigma)}{4\pi r} = \frac{1}{4\pi r}. \tag{4}$$

This is the central formula for so called "particle mesh Ewald" methods [2,3]. One neglects contributions with $\mathbf{p} \neq 0$ and calculates the Coulomb energy as a lattice energy, Eq. (1), plus a short-range correction. Deviations from Eq. (4) occur if the structure factors are not Gaussian: For splines $\tilde{f} = \Pi_\alpha \mathrm{sinc}^n(q_\alpha/2)$ with $\alpha = (x,y,z)$ which has the cumulant expansion $\tilde{f} \sim \Pi \exp(-nq_\alpha^2/24 - nq_\alpha^4/2880)$. Splines converge for large n to Gaussians of width $\sigma^2 = n/12$. However interpolation with splines generates an extra contribution at $q=0$ in Eq. (3) due to the term in q_α^4 in the cumulant. This leads in real space to an error which decays as $1/r^5$. The amplitude of this error decays rather slowly with n.

The aliasing error comes from the contributions $\mathbf{p} \neq 0$. Consider, for instance the self-energy $U(\mathbf{r},\mathbf{r})/2$ and the contribution to Eq. (2) from $\mathbf{p}_1 = (1,0,0)$. Since $\tilde{f}(\mathbf{q})$ decays rapidly in Fourier space, the product $\tilde{f}(\mathbf{q} - 2\pi\mathbf{p}_1)\tilde{f}(\mathbf{q})$ is maximum on the boundary of the first Brillouin zone near $\mathbf{q} = \pi(1,0,0)$. If we sum over all symmetry-related lattice reciprocal vectors, we find a periodic one-body potential

$$V_1 \sim \tilde{f}^2(\pi\mathbf{p}_1) G(\pi\mathbf{p}_1) \sum_\alpha \cos 2\pi r_\alpha. \tag{5}$$

Higher-order corrections to V_1 come from larger $\mathbf{p}$. We compare spline and Gaussian interpolation: For a Gaussian $\tilde{f}^2(\pi\mathbf{p}_1) = e^{-\pi^2\sigma^2}$, whereas for a n-spline we find $\tilde{f}^2 = (2/\pi)^{2n} \sim e^{-0.9n}$. Requiring $\tilde{f}^2 \sim 10^{-4}$ implies that $\sigma \sim 1$ or $n \sim 10$. An implementation using low-order splines with only $n=3$ showed strong aliasing artefacts [8]. The sinusoidal form of Eq. (5) permits simple analytic subtraction, but we will not pursue this point here.

We now turn to errors in the lattice Green function, $G(\mathbf{r})$. Coulomb's law in electromagnetism results from the imposition of a linear constraint, Gauss' law: $\nabla \cdot \mathbf{E} = \rho$, on a quadratic energy functional: $U = 1/2 \int \mathbf{E}^2 d^3\mathbf{r}$. Previous codes that discretized these equations led to the standard seven-point discretization of the Laplacian operator:

$$G^{-1}(\mathbf{q}) = 2 \sum_{\alpha=1}^{3} (1 - \cos q_\alpha) \tag{6}$$

Expanding, we find

$$G(\mathbf{q}) = \frac{1}{q^2} + \frac{1}{q^4} \sum_{\alpha=1}^{3} \frac{q_\alpha^4}{12} + \ldots \tag{7}$$

The presence of terms which involve q_α^4/q^4 imply a correction to $G(\mathbf{r})$ which decays as only $1/r^3$. We now construct a discretization which converges faster. Consider an energy which is a quadratic function of P electric field variables E_i, where the subscript includes both positional and directional information.

$$U_E = \frac{1}{2} \sum_{i,j}^{P} E_i K_{ij} E_j \equiv EKE/2 \tag{8}$$

We continue with an operator notation for compactness. We submit this energy to $L < P$ linear constraints, c_l

$$c_l \equiv \sum_{p=1}^{P} D_{lp} E_p - e_l = 0, \quad \forall\, l, \tag{9}$$

where D_{lp} is a discretization of the divergence operator at l and e_l is the charge. Stationary points are found by considering the functional $A = U_E - \Sigma_l \phi_l c_l$. D is a linear operator, we define the adjoint D^*. The variational equations of E are

$$KE - D^*\phi = 0. \tag{10}$$

Solving for E in Eq. (10) and substituting in the constraint equation Eq. (9), we find a generalized Poisson equation for the Lagrange multipliers ϕ

$$DK^{-1}D^*\phi - e = 0 \tag{11}$$

From this Poisson equation, we find that the minimum of the constrained energy is

$$U_c = e\phi/2 = eG_K e/2, \tag{12}$$

with the Green function $G_K^{-1} = DK^{-1}D^*$. We make contact with electrostatics if we recognize that $D = \mathrm{div}$ implies $D^* = -\mathrm{grad}$, and $G^{-1} = -\nabla^2$.

We will now generalize these results to nonzero temperatures and show that the effective interaction between particles is still described by the Green function G_K. The constraints are now imposed by delta-functions in a partition function

$$Z = \int \prod_{p=1}^{P} dE_p e^{-\beta U_E} \prod_{l=1}^{L} \delta(c_l), \tag{13}$$

We decompose the field E into generalized "longitudinal" and "transverse" components by writing $E = K^{-1}D^*\phi + E_t$ and change integration variables from E to E_t. The partition function then factorizes

$$Z = e^{-\beta U_c} \int \prod_{p=1}^{P} dE_{t,p} e^{-\beta E_t K E_t/2} \prod_{l=1}^{L} \delta(DE_t),$$

$$= Z_K \times \text{constant}, \tag{14}$$

where Z_K is a partition function for particles interacting with the Green function G_K.

Previous implementations [6] took the following forms for the operators D and K: DE was the flux out of the site l to the six nearest-neighbor sites. K was diagonal, $K = \delta_{ij}$, leading to Eq. (6). Here, we keep the same form for the operator D, but for K we include interactions between neighboring links on the lattice; for x-oriented bonds of the lattice the energy function is

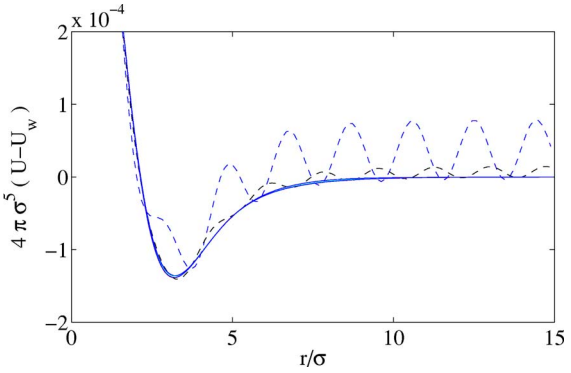

FIG. 1. (Color online) Scaled error in the pair potential using the energy Eq. (16) for $\sigma=0.90$, 1.0, 1.2, 1.4, and 1.6. One particle placed at (0, 0, 0) the second displaced in the direction (1, 1, 1). Solid lines: Curves for $\sigma=1.2$, 1.4, and 1.6 superpose: Errors in G dominate. Dashed lines: $\sigma=0.90$ and 1.0. Oscillations, Eq. (5), from aliasing are also important and violate the scaling in σ^5.

$$U_E = \frac{1}{2}\sum\left\{\frac{5}{6}E_{i,j,k|x}^2 + \frac{1}{12}E_{i,j,k|x}(E_{i+1,j,k|x} + E_{i-1,j,k|x})\right\}, \tag{15}$$

with similar expression for the links in the y and z directions. In Fourier space, we find that

$$K(\mathbf{q}) = \frac{1}{6}\,\mathrm{diag}(5+\cos q_x, 5+\cos q_y, 5+\cos q_z),$$

$$D(\mathbf{q}) = (1-e^{iq_x}, 1-e^{iq_y}, 1-e^{iq_z}),$$

$$D^*(\mathbf{q}) = (1-e^{-iq_x}, 1-e^{-iq_y}, 1-e^{-iq_z})^T,$$

where "diag" denotes a matrix with the indicated diagonal elements, so that

$$G^{-1} = D(\mathbf{q})K^{-1}(\mathbf{q})D^*(\mathbf{q}) = 12\sum_\alpha \frac{1-\cos q_\alpha}{5+\cos q_\alpha}$$

$$G(\mathbf{q}) = \frac{1}{q^2} + \frac{1}{q^4}\sum_\alpha \frac{q_\alpha^6}{240} + \ldots \tag{16}$$

This form of G leads to reduced artefacts in the lattice Green function; errors now decay as $1/r^5$.

To calibrate the effective interaction generated by our constrained algorithm, we numerically inverted the Green function Eq. (16). We take two interpolated unit charges and measured the potential between them, Fig. 1, as a function of σ and compared with the (exact) Ewald energy, U_w. We find collapse of the error when we plot $4\pi(U-U_w)\sigma^5$ as a function of r/σ for $\sigma>1$. We conclude that the error in the pair potential can be written in the scaling form

$$\delta U_G(\mathbf{r},\mathbf{r}',\sigma) = \frac{1}{\sigma^5}V_5((\mathbf{r}-\mathbf{r}')/\sigma), \tag{17}$$

for $\sigma>1$. V_5 *does* depend on the direction of the relative displacement with respect to the lattice. The error increases strongly for $r/\sigma<2$, however, smaller distances in our simulations will be within the core of the Lennard-Jones potential and will not be sampled. Due to the regularity of V_5, one could also improve accuracy of the simulation by subtracting the error off of the real space potential after parameterizing it with splines. For $\sigma<1$, aliasing errors are increasingly important, adding an sinusoidal contribution to the error as expected from Eq. (5). $\sigma=1$ generates errors in the potential which are $O(10^{-4})$.

One simulates a system described by the energy Eq. (8) with the constraint Eq. (9) with the Metropolis method by introducing two independent Monte Carlo updates: Plaquette updates, which satisfy $D\delta E=0$, consist of the coupled update of the four links forming a plaquette [6] of the cubic lattice. On each of these links, the field is modified by the same amount Δ, so that the flux of E at each node remains constant. With the addition of nearest-neighbor interactions, Eq. (15), calculation of the energy change requires the values of the field from 12 links. Motion of a particle is possible if a local update of the field is performed simultaneously such that $D\delta E=\delta\rho$ where $\delta\rho$ is the localized charge fluctuation.

We implemented a simulation of TIP3P water using Gaussian interpolation due to the superior convergence properties at higher accuracies. We work in units of the mesh size. Three-dimensional Gaussians, with $\sigma=1$, are calculated as direct products of one-dimensional Gaussians each truncated at $\lambda=4.3$. The three atoms of each molecule are interpolated together. The small error, $O(10^{-8})$, in charge conservation is corrected on the grid point nearest the oxygen atom. In this way, we insure that charge is conserved in the algorithm to machine precision. We perform a trial move and re-perform both interpolation and charge correction steps. This gives us a localized charge fluctuation $\delta\rho$. We generate a local field modification in a box enclosing the original and final sites: We use a δE such that $\Sigma_i \delta E_i^2/2$ is minimum while respecting $D\delta E=\delta\rho$. Outside of the region where $\delta\rho=0$, we impose that $\delta E=0$. This leads to a *small* Poisson problem (with zero flux boundary conditions) within the interpolation volume which can be solved using the FFTW library [9]. Lennard-Jones and erfc interactions were truncated at a distance of 9 Å. We use Monte Carlo updates in both the position and orientation of the molecules, tuned to give an acceptance rate of about 40%. For each update of a molecule, we perform 100 plaquette updates. Simulations were performed at 300 K at constant volume. Due to the simplicity of the plaquette updates compared with the the calculation of the erfc interaction, they take a small part of the simulation time.

We compared our Monte Carlo simulation of TIP3P with a molecular dynamics simulation [10] using using a Langevin thermostat, friction 1 ps^{-1}, integration time step 1 fs. We used a cubic box of side 18.62 Å and a grid of 20^3 sites for the Monte Carlo. We measured the autocorrelation time of the potential energy, V using blocking [11], after removing the energy in the transverse electric field in the Monte Carlo runs. A set of recordings corresponding to T sweeps or time steps is averaged in blocks of $b=2^m$ recordings, to estimate the mean potential energy, $\langle V\rangle$, and a running estimate in the error in $\langle V\rangle$, $\tilde{\sigma}(b)$. For large blocking factors, $\tilde{\sigma}(b)$ saturates to a constant $\tilde{\sigma}_v$; the integrated autocorrelation time is given

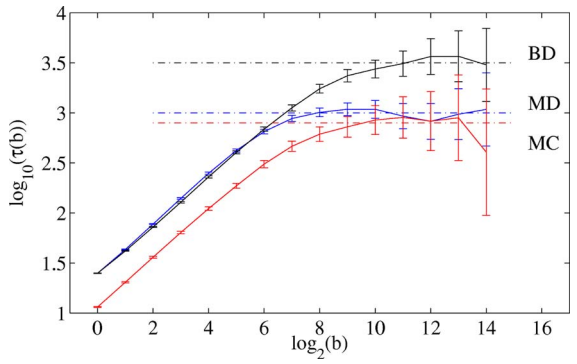

FIG. 2. (Color online) Blocking analysis of the energy with Monte Carlo (MC), molecular dynamics (MD), and Brownian dynamics (BD) to estimate the energy autocorrelation time. The estimated τ for each method is indicated with a dot-dashed line.

by $\tau=\tilde{\sigma}_v^2 T/2\langle V^2-\langle V\rangle^2\rangle$. In order to obtain good statistics for the dynamics, we simulated a small system of 216 particles for several thousand τ; use of large systems would require simulations which are too slow to give useful statistical results on dynamical quantities. The running estimate of $\tau(b)$ is plotted in Fig. 2. We estimate that $\tau=1100$ for molecular dynamics and $\tau=800$ for Monte Carlo. We also performed Brownian dynamics simulations with the time step equal to 1/10 of the stability limit using an Euler integrator finding $\tau=3200$.

To conclude, we have implemented a Monte Carlo algorithm for the simulation of TIP3P. Each Monte Carlo time step implies two interpolations per charge plus calculation of a localized current. Each molecular dynamics step requires one charge interpolation and then three extrapolations for the force plus solution of the Poisson equation. The total complexity of the interpolation steps is very similar in molecular dynamics (particularly multigrid) codes and in our Monte Carlo formulation. The integrated autocorrelation time with our algorithm is comparable to simulations performed using molecular dynamics when measured in sweeps. CPU time comparisons were less favorable to our code in part since the (Fourier-based) Gromacs package contains contains extensively optimized routines for interpolation which we did not implement. Multigrid and the present Monte Carlo algorithm are also obliged to use a larger interpolation footprint than pure Fourier-based algorithms. Improved algorithms for Gaussian interpolation will reduce the speed difference.

In this article, we introduced estimates of the error in the real-space potential generated by our algorithm. These estimates differ from those widely used in the analysis of molecular dynamics codes, which concentrate on force errors. Force estimates are, however, not natural for the analysis of Monte Carlo algorithms. If we were to implement the above discretizations in a molecular dynamics code using the ideas in Ref. [12] force errors would then be very similar to those presented in the analysis of multigrid algorithms in Ref. [3]. This paper also gives a detailed comparison of the relative errors in real space solvers such as multigrid and more conventional Fourier-based solvers.

The authors in Ref. [3] also reduced the range of the interpolation step by introducing a second on-lattice convolution after interpolating charges to the grid. Similar techniques are possible here if we modify the kernel K so as to include a extra spreading step; charge interpolation then becomes cheaper. In our algorithm, this simplification in charge motion is balanced by an increase in the complexity of plaquette updates.

Our algorithm has the important advantage over other codes of being purely local, and thus easily implemented on parallel computers with limited interprocessor communication, such as is the case on low cost clusters. With a Monte Carlo algorithm, there is also an enormous gain in flexibility in heterogenous environments: In simulations of a biomolecule or an interface most of the water molecules play the role of distant spectator, even if they provide the majority of charge centers. In Monte Carlo, it is trivial to bias moves toward interesting degrees of freedom, or even introduce cluster [13] or multistep [14] updates; with molecular dynamics multiscale and multistep algorithms are difficult to implement and prone to instability.

[1] W. L. Jorgensen, J. Chandrasekhar, J. D. Madura, R. W. Impey, and M. L. Klein, J. Chem. Phys. **79**, 926 (1983).
[2] U. Essmann, L. Perera, M. L. Berkowitz, T. Darden, H. Lee, and L. G. Pedersen, J. Chem. Phys. **103**, 8577 (1995).
[3] Y. Shan, J. L. Klepeis, M. P. Eastwood, R. O. Dror, and D. E. Shaw, J. Chem. Phys. **122**, 054101 (2005).
[4] C. Sagui and T. Darden, J. Chem. Phys. **114**, 6578 (2001).
[5] A. Duncan, R. D. Sedgewick, and R. D. Coalson, Phys. Rev. E **71**, 046702 (2005).
[6] A. C. Maggs and V. Rossetto, Phys. Rev. Lett. **88**, 196402 (2002).
[7] I. Pasichnyk and B. Dünweg, J. Phys.: Condens. Matter **16**, S3999 (2004).
[8] J. Rottler and A. C. Maggs, J. Chem. Phys. **120**, 3119 (2004).
[9] M. Frigo and S. G. Johnson, Proc. IEEE **93**, 216 (2005).
[10] E. Lindahl, B. Hess, and D. van der Spoel, J. Mol. Model. **7**, 306 (2001).
[11] H. Flyvbjerg and H. G. Petersen, J. Chem. Phys. **91**, 461 (1989).
[12] J. Rottler and A. C. Maggs, Phys. Rev. Lett. **93**, 170201 (2004).
[13] S. W. Rick and A. D. J. Haymet, J. Chem. Phys. **118**, 9291 (2003).
[14] K. Bernacki, B. Hetenyi, and B. J. Berne, J. Chem. Phys. **121**, 44 (2004).